

# **Tensile Properties of Polymeric Matrix Composites Subjected to Cryogenic Environments**

Karen S. Whitley and Thomas S. Gates

## **ABSTRACT**

Polymer matrix composites (PMC's) have seen limited use as structural materials in cryogenic environments. One reason for the limited use of PMC's in cryogenic structures is a design philosophy that typically requires a large, validated database of material properties in order to ensure a reliable and defect free structure.

It is the intent of this paper to provide an initial set of mechanical properties developed from experimental data of an advanced PMC (IM7/PETI-5) exposed to cryogenic temperatures and mechanical loading. The application of this data is to assist in the materials down-select and design of cryogenic fuel tanks for future reusable space vehicles. The details of the material system, test program, and experimental methods will be outlined. Tension modulus and strength were measured at room temperature,  $-196^{\circ}\text{C}$ , and  $-269^{\circ}\text{C}$  on five different laminates. These properties were also tested after aging at  $-186^{\circ}\text{C}$  with and without loading applied. Microcracking was observed in one laminate.

## **BACKGROUND**

The literature provides limited experimental data on the strength, stiffness, and durability of PMC's operating at cryogenic temperatures. In the work by Pannkoke [1], tests were performed to determine the fatigue behavior of unidirectional thermoplastic composites at  $-196^{\circ}\text{C}$ . The fatigue strength was found to be only 60% of the static strength at  $10^6$  cycles. In this work, it was recognized that large thermal stresses degraded the fatigue performance. In a series of articles by Pannkoke [2] and Alhborn [3], static and cyclic thermal/mechanical tests were performed on unidirectional and cross-ply thermoplastic composites. Isothermal tests were performed at  $23^{\circ}\text{C}$ ,  $-196^{\circ}\text{C}$ , and  $-269^{\circ}\text{C}$  and cyclic thermal tests were determined between  $-196^{\circ}\text{C}$  and  $23^{\circ}\text{C}$ . Strength, damage, and fatigue life were measured for all test conditions. It was found that the effects of temperature on

static strength were largely related to the matrix dominated properties, shear and transverse tension, and that increases in matrix dominated strength as temperature decreased could be offset by the development of thermal-stress induced cracks. As in previous studies, the fatigue life was reduced as the test temperature was decreased. More recently, a compilation of test data [4], for several PMC material systems showed that in general, tensile modulus, tensile strength, and compressive strength all increased as the test temperature was decreased from 23°C to -269°C. Once again, it was found that thermal stresses had a large influence on behavior and that the sensitivity of matrix-dominated properties to temperature can be used to help explain the stress-strain response of laminated composites.

### **Application of PMC'S to Cryogenic Fuel Tanks**

As the demands on performance increase for future space transportation vehicles, the need for efficient, lighter weight structures will also continue to increase. For liquid fueled rocket engines, one area identified as a potential source for significant weight reduction is the replacement of metallic cryogenic fuel tanks with PMC tanks. This is a demanding application for PMC's because a typical cryogenic fuel tank wall must carry structural and pressure loads while safely operating over an extremely wide temperature range (e.g. -250°C to +120°C).

The interest in design of polymeric composite cryogenic-fuel tanks for spacecraft goes back several years to research associated with the National Aerospace Plane (NASP) and the single-stage-to-orbit (SSTO) vehicles [5], [6]. It was recognized that fuel containment or permeation resistance of the tanks could be the overriding design criteria.

More recently, in 1996, the DC-XA suborbital demonstration vehicle was built with an all-composite liquid-hydrogen fuel tank [7]. That tank was designed as an unlined, unstiffened cylinder measuring approximately 2.4 m in diameter. The tank performed as expected in both ground and flight tests. Although long-term use of the tank was not investigated, short-term testing indicated that permeation resistance and structural load carrying capability met the design requirements.

For long-term applications such as dictated by manned, reusable launch vehicles, an efficient cryo-tank design must ensure a safe and reliable operating environment. To execute this design, extensive experimental data must be collected on the lifetime durability of PMC's subjected to realistic thermal and mechanical environments. This experimental data should establish the basic material response and provide a complete set of material properties that can be used in both analysis and design. It is the intent of this paper to provide an initial set of material property data and associated test methods for PMC cyro-tank structures.

### **MATERIAL SYSTEM**

The PMC material used in this study, IM7/PETI-5, consisted of a continuous high strength, intermediate modulus, carbon fiber in a thermoplastic polyimide matrix. All test materials were laminated composites fabricated at the NASA Langley Research Center. These composite panels consisted of unidirectional and angle-ply

laminates,  $([0]_{12}, [90]_{12}, [\pm 65]_{3s}, [\pm 45]_{3s})$ , and a 13 ply quasi-orthotropic laminate  $([45/90_3/-45/\bar{0}_3]_s)$ . The bar notation over the 0 indicates that the  $0_3$  group is not symmetric. Figure 1 provides a schematic illustrating the coordinate system for the fiber orientations relative to the specimen dimensions.

These lay-ups were chosen to provide basic lamina-level material constants and in the case of the  $[\pm 65]_{3s}$  and  $[45/90_3/-45/\bar{0}_3]_s$  laminates, to be representative of a composite wall in a typical cryogenic propellant tank. For a cryo-tank, the orientation of the  $0^\circ$  ply in the  $[45/90_3/-45/\bar{0}_3]_s$  laminate would be in the longitudinal axis direction of the tank.

All composite panels were fabricated by hand lay-up. The bagging and cure processes employed were consistent with standard practices. Through-transmission, ultrasonic inspection indicated that there were no significant internal anomalies in any of the panels. The glass transition temperature ( $T_g$ ) of the as-received composite material was  $267^\circ\text{C}$  as measured by the peak in the tan delta curve of tests run in a dynamic mechanical analysis (DMA) test [8].

## MATERIAL CHARACTERIZATION

The material characterization test plan consisted of two phases. The first phase addressed material aging. In this phase the material was subjected to long-term exposure at cryogenic temperature in either an unloaded or statically loaded state. The second phase was residual property characterization of aged and unaged specimens at three temperatures ( $23^\circ$ ,  $-196^\circ$ ,  $-269^\circ\text{C}$ ). This phase provided fundamental material properties and an understanding of material behavior as a function of prior aging conditions and test temperatures. The complete test matrix including the phase one aging conditions and the phase two residual property tests are shown in table I.

**TABLE I. TEST MATRIX**

Test Temp ( $^\circ\text{C}$ )	Aging Condition ( $-184^\circ\text{C}$ )		
	No Load	Static Load (3000 $\mu\text{E}$ )	Static Load (4000 $\mu\text{E}$ )
23	$[0]_{12}, [90]_{12}, [\pm 45]_{3s}, [\pm 65]_{3s}, [45/90_3/-45/\bar{0}_3]_s$	$[\pm 45]_{12}, [0]_{12}$	$[\pm 65]_{3s}, [45/90_3/-45/\bar{0}_3]_s$
-196	$[0]_{12}, [90]_{12}, [\pm 45]_{3s}, [\pm 65]_{3s}, [45/90_3/-45/\bar{0}_3]_s$	$[\pm 45]_{12}, [0]_{12}$	$[\pm 65]_{3s}, [45/90_3/-45/\bar{0}_3]_s$
-269	$[0]_{12}, [90]_{12}, [\pm 45]_{3s}, [\pm 65]_{3s}, [45/90_3/-45/\bar{0}_3]_s$	$[\pm 45]_{12}, [0]_{12}$	$[\pm 65]_{3s}, [45/90_3/-45/\bar{0}_3]_s$

All tests were conducted on coupon type test specimens that were cut from the larger panels prior to aging. A schematic of the test coupon is presented in figure 1.

The general set of references for the residual tension test is SACMA SRM 4-88 and ASTM D 3039-76. Data reduction on all residual mechanical property tests was done in accordance with the individual test standards. A basic description of each type of test is provided below. The modulus was calculated using ASTM D3039-76 and a linear regression least squares curve fit of the stress/strain data in the linear region. The linear region of the stress/strain curve was most commonly defined as being between 1000 and 3000 $\mu\epsilon$ .

### **Test Phase One - Material Aging**

A unique test fixture developed under the NASA High Speed Research Program [9] and fabricated at Northrop-Grumman Corp. was used to produce a constant strain condition during the aging phase. Each fixture, shown in figure 2, was constructed of Invar material (CTE=1.4  $\mu$  mm/mm  $^{\circ}$ C) and could accommodate two rectangular specimens. Each specimen was individually preloaded to the desired strain level by compressing a series of spring-type washers that reacted against the frame and put the specimen into tension. As the specimen was preloaded and the washers were tightened, the strain in the specimen was monitored with a longitudinal extensometer mounted on the specimen.

The preload strain level, given in table I, was selected to be approximately 50% of the room temperature failure strain. The high stiffness of the fixture relative to the test specimen and the low CTE of the Invar material ensured a constant strain condition over the entire aging period. During the course of a typical aging phase, 13 of these constant strain fixtures were placed into a large cryo-chamber that maintained a constant temperature of  $-184^{\circ}$ C for 24 days.

### **Test Phase Two - Residual Properties**

In phase two of the test program, residual strength and stiffness were measured after aging. All residual property tests were performed in tension on a servo-hydraulic test machine using a loading rate of 1.27 mm/min. The isothermal cryogenic conditions at  $-196^{\circ}$ C and  $-269^{\circ}$ C were achieved by immersing the test specimen and load introduction apparatus into liquid nitrogen or liquid helium respectively. In order to reach thermal equilibrium, the specimen stayed immersed in a constant level of the cryogen for at least 15 minutes prior to mechanical loading.

Stress in the test specimens was calculated using load, as measured by the test machine load cell, divided by the original cross section of the specimen. Failure load was defined as the point of complete loss of load carrying capability.

Strain in the test specimen was measured using combinations of cryogenic-rated axial extensometers (MTS model 634.11F-21) and bonded electrical resistance strain gages (Measurements Group WK-00-250BG-350). Temperature compensation was achieved by zeroing the extensometer and gages after the

specimen reached thermal equilibrium. Details on these techniques can be found in [10]. Placement of these sensors on the specimen is shown in figure 1.

Prior to the destructive residual tests, visual examination of all lay-ups was used to determine if the exposure conditions generated any microcrack damage. A microcrack was defined as a transverse or longitudinal crack, observable under at least 25x magnification, which was at least one ply thickness in length. Prior to aging exposure, representative samples were polished along one edge and photomicrographs were taken to establish the baseline condition. Based on the data in the literature ([1] - [4]) it was expected that microcrack damage could even occur as a result of the cure process itself when the large change in temperature from the stress-free cure temperature to room temperature would induce interlaminar stresses. Microphotographs representative of the specimen's edge before and after aging are shown in figure 3.

## RESULTS AND DISCUSSION

TABLE II contains elastic modulus and strength values at the three different test temperatures for each lay-up for the not aged material, and the aged material with and without load. Each number represents the average of three replicates. These results are represented graphically in figures 4-9 where the error bars show the maximum and minimum value of the three replicates.

**TABLE II. MODULUS AND STRENGTH VALUES**

Lay-up	Temp °C	Not Aged		Aged Without Load		Aged With Load	
		Elastic Modulus (GPa)	Strength (MPa)	Elastic Modulus (GPa)	Strength (MPa)	Elastic Modulus (GPa)	Strength (MPa)
[0]	24	157.6	1939.8	153.6	1864.8	147.2	1847.8
	-196	151.6	1277.9	146.3	1567.7	149.2	1536.1
	-269	145.1	1495.2	143.0	1451.0	158.6	1771.4
[±65]	24	71.9	1132.2	70.3	1265.9	59.8	954.9
	-196	75.7	911.6	63.8	902.4	71.5	1119.5
	-269	73.1	1130.7	69.4	1113.6	65.6	1024.4
[45/90 <sub>3</sub> /-45/ $\bar{0}$ <sub>3</sub> ] <sub>s</sub>	24	50.7	711.0	46.7	699.9	51.0	842.6
	-196	40.6	585.4	48.0	747.9	48.6	872.4
	-269	43.8	656.5	44.3	731.8	52.4	806.1
[±45]	24	16.6	334.0	18.1	371.8		
	-196	20.9	246.7	21.6	255.8		
	-269	21.7	258.3	20.4	257.7	20.6	257.0
[90]	24	8.7	46.7	8.6	46.6		
	-196	7.5	21.0	9.6	58.3		

## Effects Of Temperature

### NOT AGED SPECIMENS

The modulus of the not aged  $[0]_{12}$  and  $[45/90_3/-45/\bar{0}_3]_s$  lay-ups decreased as the temperature decreased, whereas the off-axis lay-ups,  $[\pm 65]_{3s}$  and  $[\pm 45]_{3s}$  experienced an increase in modulus as the temperature decreased. The strength values at  $-269^\circ\text{C}$  were lower than those at room temperature, however the lowest strength values occurred at  $-196^\circ\text{C}$  for all lay-ups.

### AGED WITHOUT LOAD SPECIMENS

Temperature did not have a significant impact on the modulus of the aged-without-load material. The  $[0]_{12}$  and  $[\pm 65]_{3s}$  specimens showed a slight decrease in modulus in going from room temperature to  $-196^\circ\text{C}$ , whereas the  $[45/90_3/-45/\bar{0}_3]_s$ ,  $[\pm 45]_{3s}$ , and  $[90]_{12}$  showed a slight increase. The strength of the material aged without load tended to decrease as the temperature decreased for all lay-ups except the  $[45/90_3/-45/\bar{0}_3]_s$ .

### AGED WITH LOAD SPECIMENS

In the case of the specimens aged-with-load, the modulus of the  $[0]_{12}$  increased as temperature decreased. The  $[\pm 65]_{3s}$  had the highest modulus at  $-196^\circ\text{C}$ . The modulus of the  $[45/90_3/-45/\bar{0}_3]_s$  did not change significantly as function of temperature.

The strength of the aged-with-load material was not significantly different at  $-269^\circ\text{C}$  than the strength values at room temperature. The most significant change in strength among the three lay-ups occurred in the  $[0]_{12}$ , which experienced a 17% drop in strength at  $-196^\circ\text{C}$ .

## Effects of Aging Without Load

In general the material aged-without-load experienced lower modulus values than the not aged material. The exception was the modulus of the aged-without-load  $[45/90_3/-45/\bar{0}_3]_s$  that increased 18% from the not aged  $[45/90_3/-45/\bar{0}_3]_s$ .

Conversely, the strength of the aged-without-load material increased in several of the cases. The most significant increase was seen in the  $[0]_{12}$  and  $[45/90_3/-45/\bar{0}_3]_s$  at  $-196^\circ\text{C}$ . The  $[0]_{12}$  and the  $[45/90_3/-45/\bar{0}_3]_s$  increased 22% and 28% respectively from the not aged condition to the aged-without-load condition.

## Effects of Aging With Load

The modulus of the material that was aged with load experienced a slight drop in most cases compared to the modulus of the unaged material. The exception was

again the  $[45/90_3/-45/\bar{0}_3]_s$  in which the modulus showed a 20% increase from the not aged material at both  $-196^\circ\text{C}$  and  $-269^\circ\text{C}$ .

The most significant changes in strength of the aged-with-load material occurred at  $-196^\circ\text{C}$ . The strength increased for the three lay-ups tested with  $[45/90_3/-45/\bar{0}_3]_s$  showing the most affected increase of 49% from the not aged condition.

### **Microcracking**

The  $[45/90_3/-45/\bar{0}_3]_s$  was the only lay-up to have microcracks prior to aging indicating that this particular laminate configuration is sensitive to the processing procedure. The other lay-ups did not have cracks before aging or after aging with or without load. A microscopic examination of the  $[45/90_3/-45/\bar{0}_3]_s$  has shown that there was not a significant change to the extent of microcracking due to aging. It is believed that the ply grouping of the ortho-A material generates thermal stresses that are sufficient to cause microcracking after processing. Because of the change in material properties and the presence of microcracks, the  $[45/90_3/-45/\bar{0}_3/-45/90_3/45]$ , may be more susceptible to permeation and not a suitable lay-up for long-term use in a cryogenic fuel tank.

### **CONCLUSIONS**

Five different laminate configurations of IM7/PETI-5 were evaluated for tensile strength and stiffness at three test temperatures after being aged with and without load. Specimens were also examined for evidence of microcracking before and after aging.

In the not aged material, strength was more sensitive than modulus to test temperatures. Strength values were lower at  $-196^\circ\text{C}$  than they were at  $-269^\circ\text{C}$ . Therefore, extrapolating data beyond  $-196^\circ\text{C}$  to predict the effect of lower operating temperatures would result significant errors.

The  $[45/90_3/-45/\bar{0}_3]_s$  was the lay-up most affected by aging at  $-184^\circ\text{C}$  for 24 days without load. At  $-196^\circ\text{C}$  the modulus dropped 16%, and the strength increased 28% compared to from the not aged condition. Aging with load had the greatest effect on the modulus of the  $[0]_{12}$  and  $[45/90_3/-45/\bar{0}_3]_s$  laminate at  $-269^\circ\text{C}$ . The modulus values of  $[0]_{12}$  and  $[45/90_3/-45/\bar{0}_3]_s$  laminate increased 11% and 18%, respectively, from the modulus values of the aged-without-load specimens. In several cases the aging with load resulted in greater strength values than those of the unloaded specimens. Thus in some cases, aging-without-load tended to be more damaging than aging with load.

The microcracks seen in the  $[45/90_3/-45/\bar{0}_3]_s$  that may be due to thermal stresses in the ply grouping could render this lay-up to permeation and therefore make it unsuitable for long-term use in a cryogenic fuel tank.

## REFERENCES

1. Pannkoke, K. and H.J. Wagner, *Fatigue properties of unidirectional carbon fibre composites at cryogenic temperatures*. Cryogenics, 1991. **31**: pp. 248-251.
2. Ahlborn, K., *Durability of carbon fibre reinforced plastics with thermoplastic matrices under cyclic mechanical and cyclic thermal loads at cryogenic temperatures*. Cryogenics, 1991. **31**: pp. 257-260.
3. Ahlborn, K., *Cryogenic mechanical response of carbon fibre reinforced plastics with thermoplastic matrices to quasi-static loads*. Cryogenics, 1991. **31**: pp. 252-256.
4. Schutz, J.B., *Properties of composite materials for cryogenic applications*. Cryogenics, 1998. **38**(1): pp. 3-12.
5. Callaghan, M.T., *Use of resin composites for cryogenic tankage*. Cryogenics, 1991. **31**: pp. 282-287.
6. Robinson, M.J., *Composite Cryogenic Propellant Tank Development*. in *35th Structures, Structural Dynamics, and Materials Conference*. 1994. Hilton Head, South Carolina.
7. Robinson, M.J., *Composite Structures on the DC-XA Reusable Launch Vehicle*. in *28th International SAMPE*. 1996. Seattle, Washington.
8. Kampf, G., *Characterization of Plastics by Physical Methods, Experimental Techniques and Practical Application*. 1986, Munich: Hanser.
9. *U.S. Supersonic Commercial Aircraft*, in *Committee on High Speed Research Aeronautics and Space Engineering Board*, N.R. Council, Editor. 1997, National Academy Press: Washington, D.C.
10. Dally, J.W. and W.F. Riley, *Experimental Stress Analysis*. second ed. 1978, New York: McGraw-Hill Book Company.

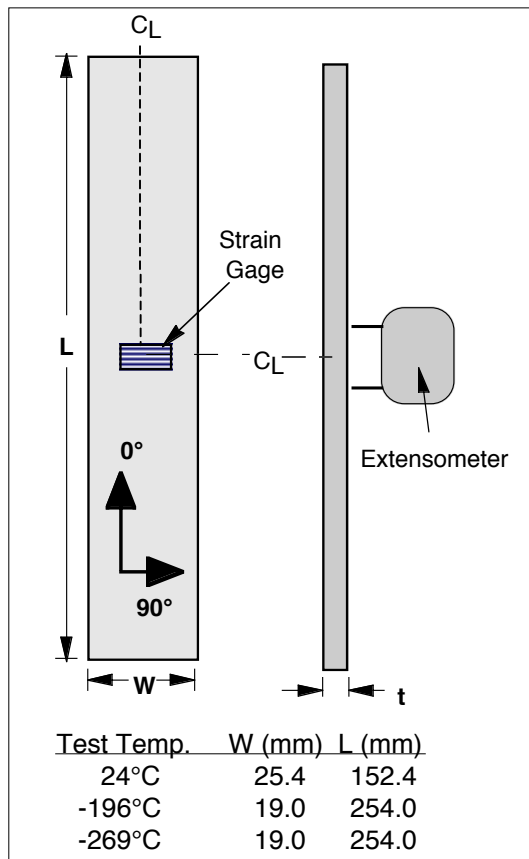


FIGURE 1. Schematic of test specimen.

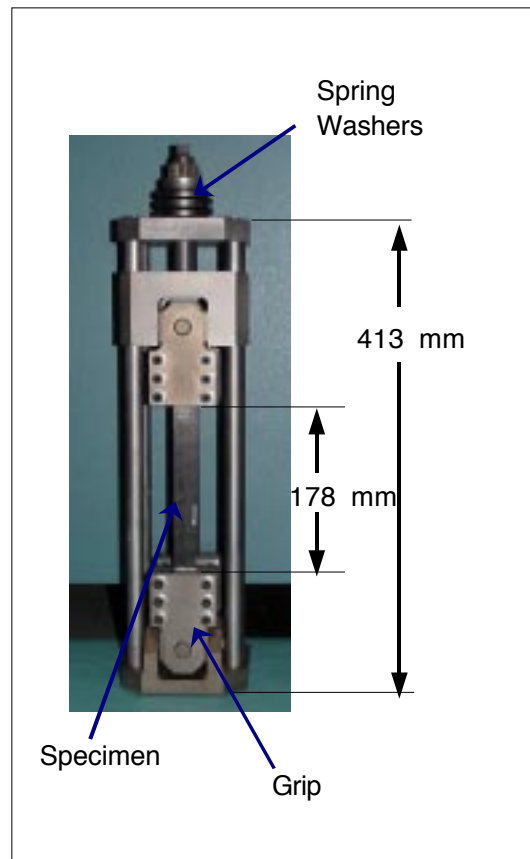


FIGURE 2. Constant strain aging fixture.

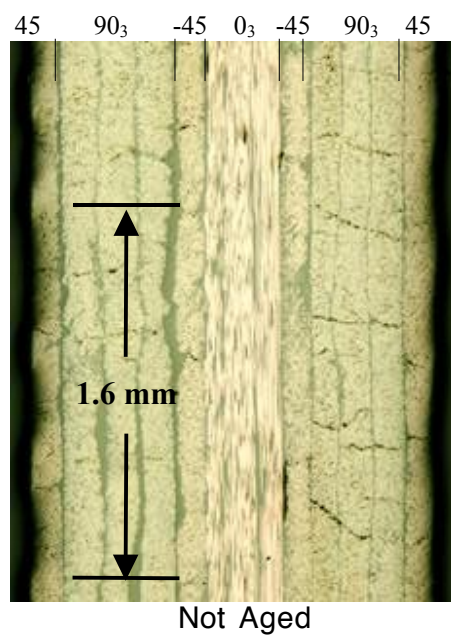


FIGURE 3. Edge of  $[45/90_3/-45/\bar{0}_3]_s$  laminates showing microcracks.

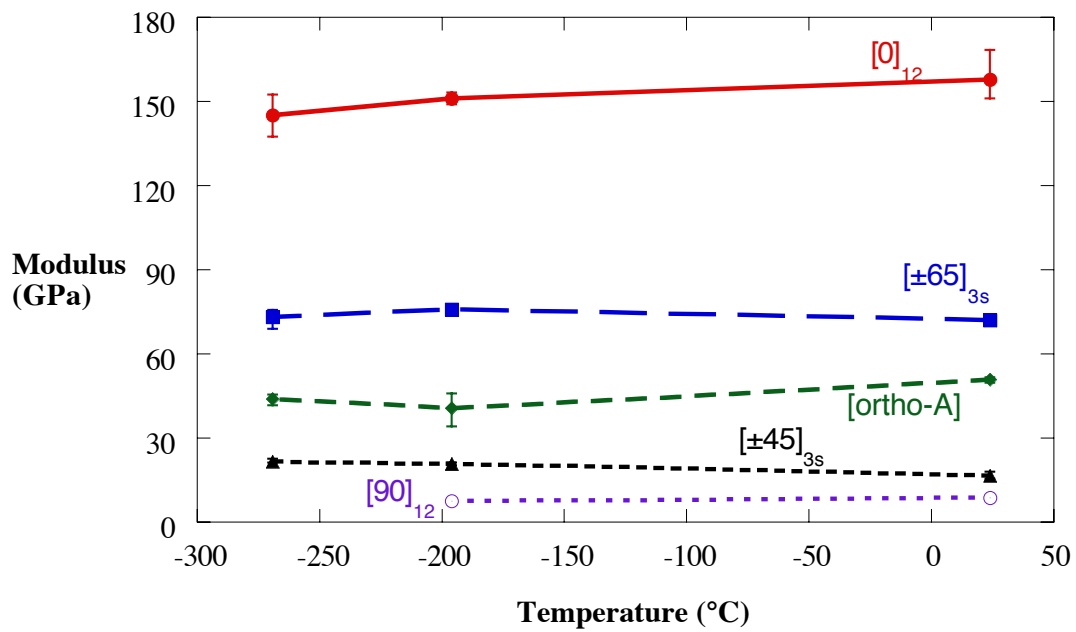


FIGURE 4. Modulus of not aged IM7/PETI-5.

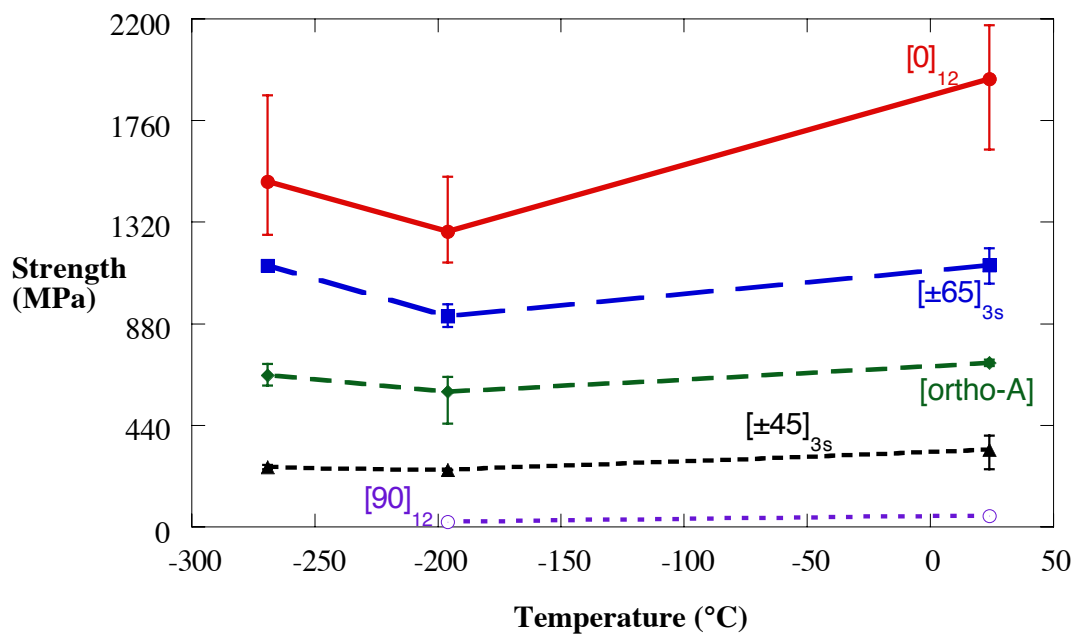


FIGURE 5. Strength of not aged IM7/PETI-5.

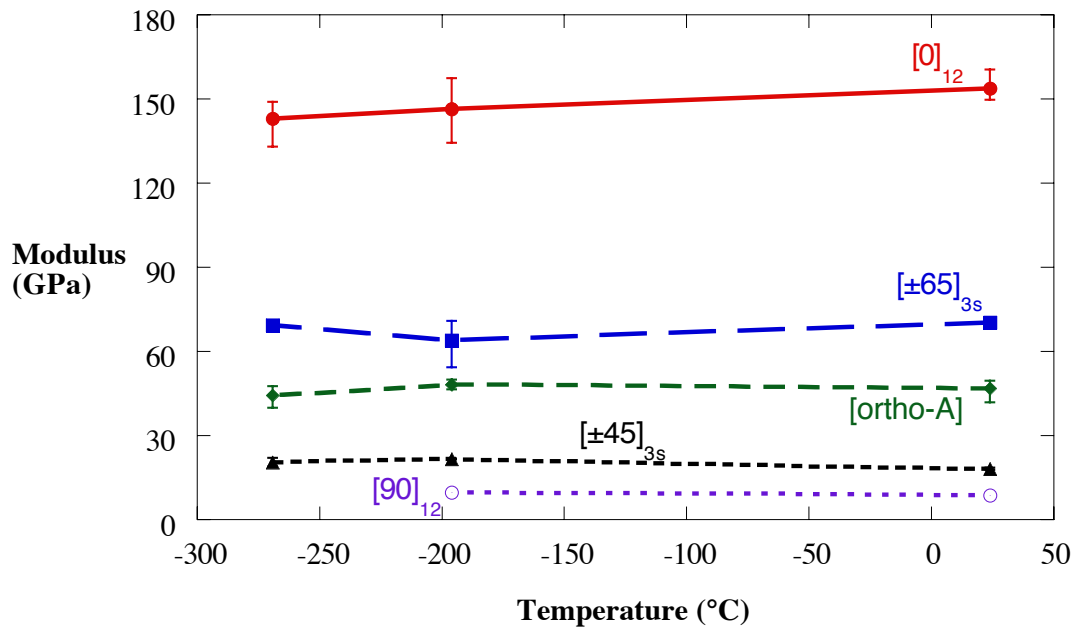


FIGURE 6. Modulus of IM7/PETI-5 aged without load at  $-184^{\circ}\text{C}$  for 24 days.

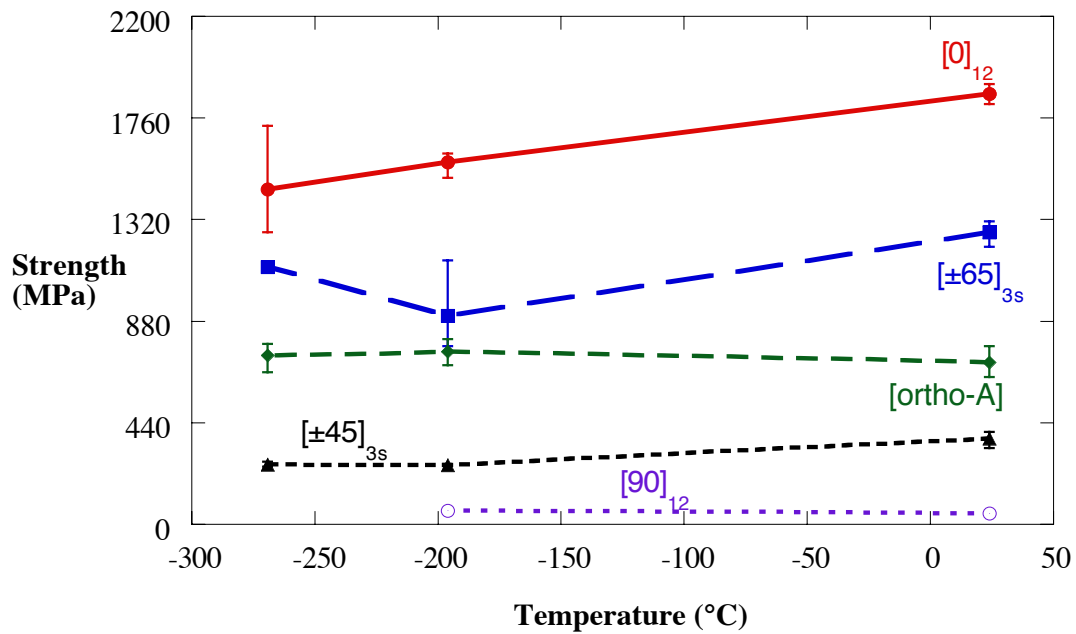


FIGURE 7. Strength of IM7/PETI-5 aged without load at  $-184^{\circ}\text{C}$  for 24 days.

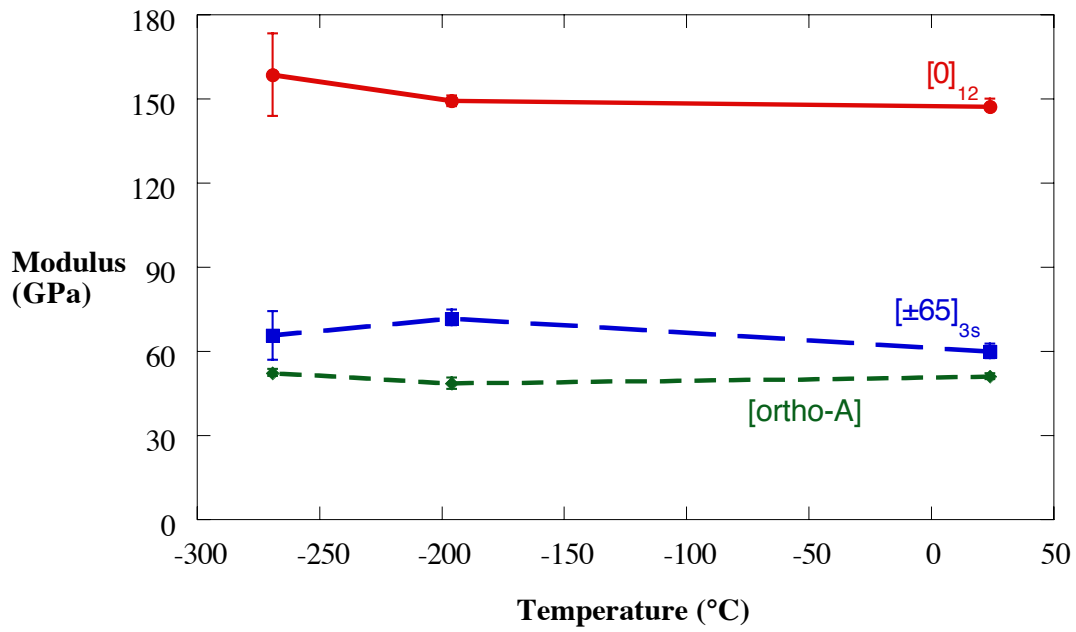


FIGURE 8. Modulus of IM7/PETI-5 aged with load at  $-184^{\circ}\text{C}$  for 24 days.

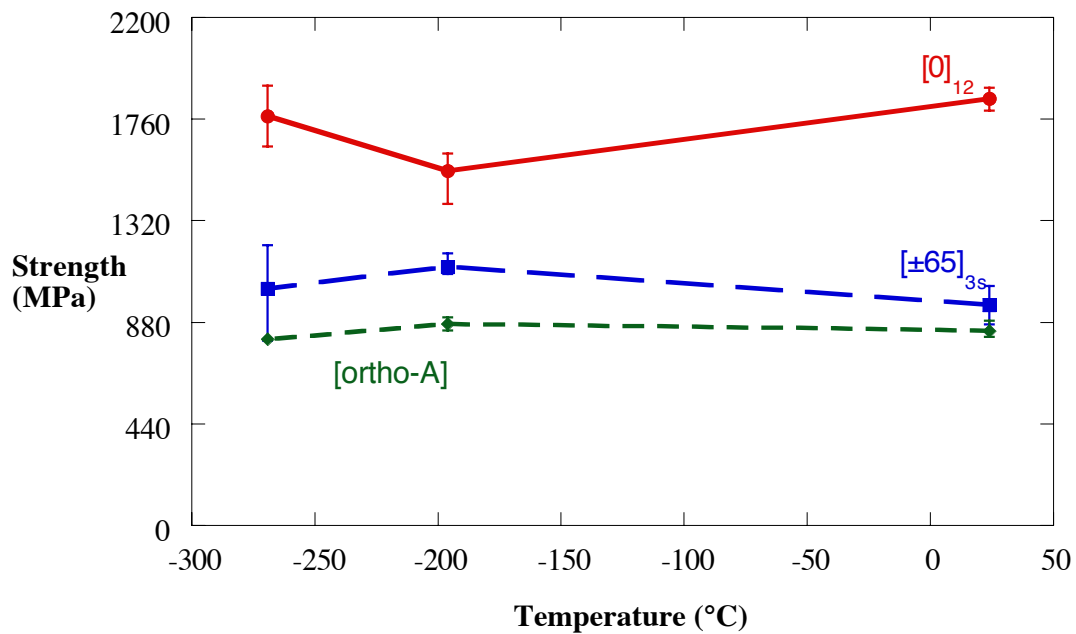


FIGURE 9. Strength of IM7/PETI-5 aged with load at  $-184^{\circ}\text{C}$  for 24 days.